

“© 2022 IEEE. Personal use of this material is permitted. Permission from IEEE must be obtained for all other uses, in any current or future media, including reprinting/republishing this material for advertising or promotional purposes, creating new collective works, for resale or redistribution to servers or lists, or reuse of any copyrighted component of this work in other works.”

# Development of Electrically Small, Bandwidth Enhanced, Vertically Polarized Filtennas

Piao Guo<sup>1</sup>, Ming-Chun Tang<sup>1</sup>, Dajiang Li<sup>1</sup>, Kun-Zhi Hu<sup>2</sup>, Richard W. Ziolkowski<sup>3</sup>

<sup>1</sup> School of Microelectronics and Communication Engineering, Chongqing University, Chongqing, China  
tangmingchun@cqu.edu.cn

<sup>2</sup> College of Automation, Chongqing University of Posts and Telecommunications, Chongqing, China  
hukz@cqupt.edu.cn

<sup>3</sup> Global Big Data Technologies Centre, University of Technology Sydney, Ultimo NSW 2007, Australia  
Richard.Ziolkowski@uts.edu.au

**Abstract**— Electrically small, bandwidth enhanced, vertically polarized omnidirectional and endfire radiating filtennas are presented. They are enabled with two hybrid  $\lambda/4$  open-circuit stubs that not only produce radiation nulls at both the upper and lower band-edges to sharpen the roll-off rate, but they also introduce an additional in-band resonance without affecting the original radiating mode. The operational bandwidth is improved significantly by the presence and overlapping of these two resonant modes. The prototypes were fabricated, assembled, and tested. The measured results are in good agreement with their simulated values and demonstrate that the omnidirectional filtenna exhibited a fractional bandwidth (FBW) of 11.3%, a peak realized gain of 3.01 dBi and an electrically small size with  $ka = 0.73$ . The endfire filtenna, which is electrically small with  $ka = 0.93$ , attained a 12.8% FBW and a peak realized gain of 6.09 dBi.

**Keywords**—Bandwidth enhanced, electrically small antenna, filtenna, vertically polarized

## I. INTRODUCTION

Vertically polarized (VP) antennas are preferred in many wireless applications because they suffer smaller attenuation loss when the electromagnetic waves they radiate propagate along a lossy medium in comparison to horizontally polarized (HP) antennas [1]. Filtennas, which seamlessly integrate the antennas and filters together into a single module, have recently experienced high interest because of their compact size and low loss advantages. Consequently, VP filtennas would be of particular interest since they would share both the attractive antenna advantages and filtering performance. However, previous works have mainly focused on HP filtenna designs [2]-[6]. Although there is one VP design previously reported in [7], it has an intrinsically high profile and an electrically large size, making it unsuitable for many low-profile, space-limited wireless platforms.

In this work, we report electrically small, bandwidth enhanced, omnidirectional and endfire radiating VP filtennas. Both filtennas have comparable wide bandwidths. Moreover, both exhibit a flat realized gain response over them and excellent frequency selectivity at their edges. A prototype of each filtenna was designed, fabricated, and measured. The measured results are in good agreement with their simulated values and verify the efficacy of both filtennas.

## II. OMNIDIRECTIONAL, ELECTRICALLY SMALL, VP FILTENNA

### A. Configuration

The omnidirectional VP filtenna is illustrated in Fig. 1. It consists of two substrates, two copper posts, and a metal ground plane. Rogers RO4003 substrates with 0.813 mm thickness, a relative dielectric constant of 3.55, and loss tangent of 0.0027, were selected for this design. The two ends of the driven post are connected, respectively, to the bottom surface of the top-hat and to the inner conductor of the SMA connector. The shorting post penetrates through both substrates to connect the top-hat directly to the ground plane. In order to improve the out-of-band selectivity, two  $\lambda/4$  open-circuit stubs (Stub 1 and Stub 2) with different lengths are etched on the top surface of the lower substrate. Their top arcs are pointed in opposite directions to achieve a more compact size, and both are connected directly to the center conductor of the 50  $\Omega$  coaxial feed.

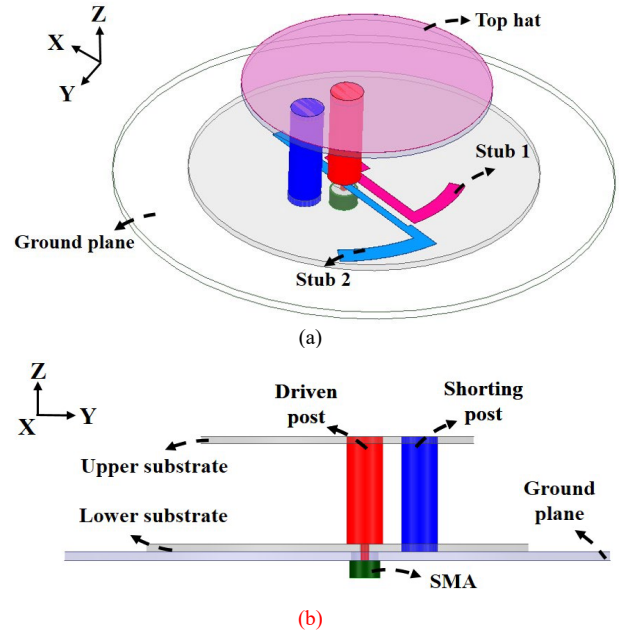


Fig. 1 The configuration of the omnidirectional VP filtenna. (a) 3-D isometric view. (b) Side view.

### B. Simulated and measured results

The optimized omnidirectional VP filtenna in Fig. 1 was fabricated, assembled, and tested. The prototype's pieces and the assembled prototype under test are shown in Fig. 2. The simulated and measured reflection coefficient and realized gain values are presented in Fig. 3. The measured  $-10$  dB impedance bandwidth is 210 MHz from 1.76 to 1.97 GHz, giving the fractional bandwidth FBW = 11.3%. The measured peak gain was 3.01 dBi. Both results are in good agreement with their corresponding simulated values. Two radiation nulls, which were introduced by the two  $\lambda/4$  open-circuit stubs, occur at 1.52 and 2.28 GHz. They produce sharp band edge skirts and high suppression levels outside of the operating band.

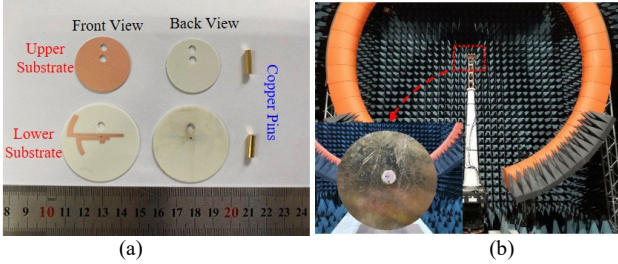


Fig. 2 Fabricated omnidirectional VP filtenna. (a) Front and back views of each layer before assembly. (b) Antenna under test (AUT) in the anechoic chamber.

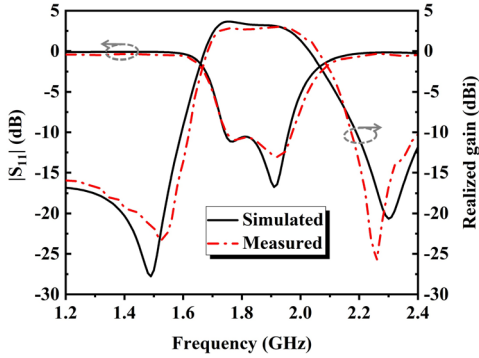


Fig. 3 Simulated and measured reflection coefficients  $|S_{11}|$  and realized gain values of the proposed omnidirectional VP filtenna.

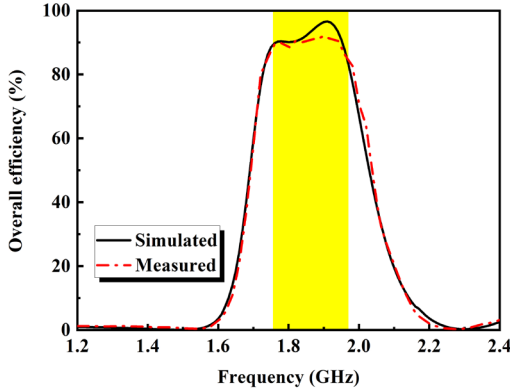


Fig. 4 Simulated and measured overall efficiency values of the realized omnidirectional VP filtenna.

The simulated and measured overall efficiencies are presented in Fig. 4. The measured (simulated) values are higher than 83% (85%) over the entire operating bandwidth. Fig. 5 presents the simulated and measured normalized realized gain patterns in the two principal planes at the center frequency, 1.85 GHz. They are in very good agreement. It is clear that the  $H$ -plane pattern is omnidirectional. The measured co-polarized fields are at least 14 dB stronger than their cross-polarized counterparts.

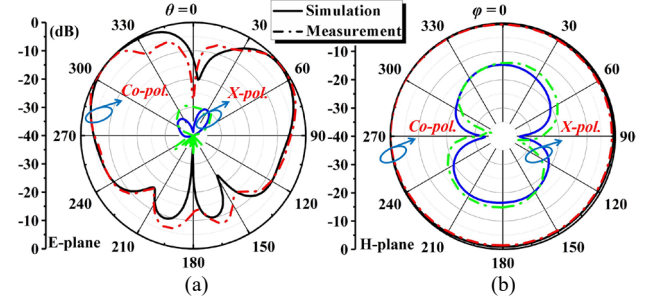


Fig. 5 Simulated and measured normalized realized gain patterns of the VP filtenna operating at 1.85 GHz. (a)  $E$ -plane ( $\phi = 270^\circ$ ). (b)  $H$ -plane ( $\theta = 50^\circ$ ).

### III. ENDFIRE RADIATING, ELECTRICALLY SMALL, VP FILTENNA

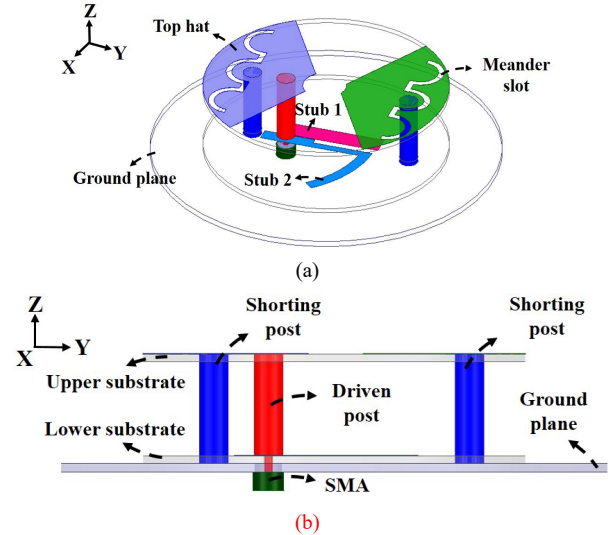


Fig. 6 The configuration of the endfire radiating, VP filtenna. (a) 3-D isometric view. (b) Side view.

#### A. Configuration

To further verify the universal usefulness of the hybrid quarter wavelength open-end stubs, another interesting electrically small VP filtenna was developed with them that radiates in the end-fire direction. Its quasi-Yagi configuration is shown in Fig. 6. A fan-shaped top-hat folded monopole acts as a director and a near-field resonant parasitic (NFRP) fan-shaped top-hat monopole serves as a reflector. They are juxtaposed to yield endfire radiated fields [8]-[9]. The two parallel  $\lambda/4$  open-circuit stubs are again printed on the upper surface of the lower substrate and are connected to the center

conductor of the coax. They significantly improve the out-of-band suppression levels.

### B. Simulated and measured results

The prototype of the optimized endfire radiating VP filtenna is shown in Fig. 7. Fig. 8 shows the simulated and measured  $|S_{11}|$  and realized gain values. The  $-10$  dB impedance bandwidth was 260 MHz from 1.9 to 2.16 GHz, a FBW of 12.8%. Furthermore, the maximum realized gain is 6.09 dBi. Two radiation nulls are observed at 1.84 and 2.5 GHz; they improve the roll-off rates and stop-band rejection levels. The measured values agree well with their simulated ones. Fig. 9 indicates that the measured (simulated) overall efficiency values are higher than 78% (80%) over the entire passband.

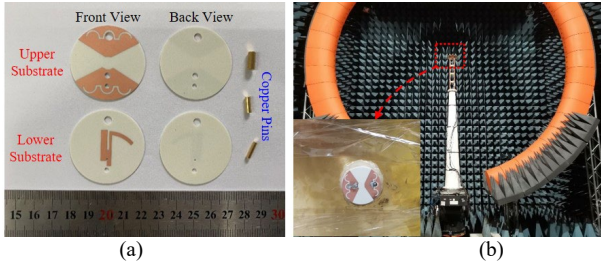


Fig. 7 Fabricated endfire radiating VP filtenna. (a) Front and back views of each layer before assembly. (b) AUT in the anechoic chamber.

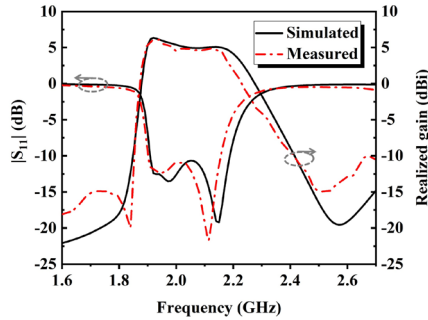


Fig. 8 Simulated and measured  $|S_{11}|$  and realized gain values of the endfire radiating VP filtenna.

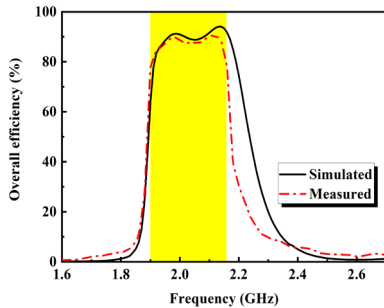


Fig. 9 Simulated and measured overall efficiency values of the endfire radiating VP filtenna.

The simulated and measured normalized realized gain patterns in the E- and H-plane are shown in Fig. 10 at the center frequency of 2.05 GHz. The endfire radiating characteristic is clearly observed in the H-plane patterns.

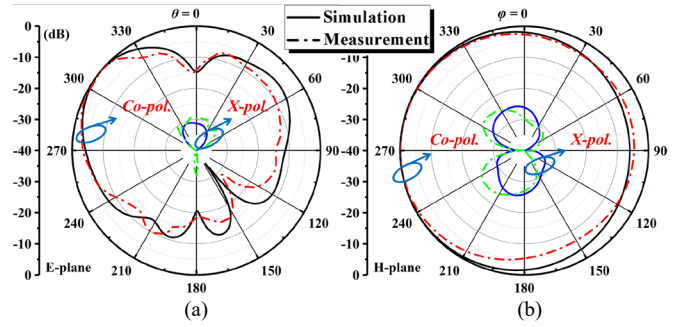


Fig. 10 Simulated and measured normalized realized gain patterns of the endfire radiating VP filtenna operating at 2.05 GHz. (a) E-plane ( $\varphi = 270^\circ$ ). (b) H-plane ( $\theta = 50^\circ$ ).

## IV. CONCLUSION

Electrically small, wide bandwidth, omnidirectional and endfire radiating VP filtennas have been designed and tested. Two  $\lambda/4$  open-circuit stubs were utilized to enhance their bandwidths and to improve their frequency selectivity. Previously reported filtennas are HP and electrically large. These two filtennas are VP, electrically small in size, and have comparable large FBWs. These advantages make them suitable for many space-limited wireless systems.

## ACKNOWLEDGMENTS

This work was supported in part by the National Natural Science Foundation of China under Contract 62061006, and in part by the Chongqing Natural Science Foundation under Contract cstc2019jcyjqqX0004.

## REFERENCES

- [1] J. Liu and Q. Xue, "Microstrip magnetic dipole Yagi array antenna with endfire radiation and vertical polarization," *IEEE Trans. Antennas Propag.*, vol. 61, no. 3, pp. 1140–1147, Mar. 2013.
- [2] K.-Z. Hu, M.-C. Tang, Mei Li, and Richard W. Ziolkowski, "Compact, low-profile, bandwidth-enhanced substrate integrated waveguide filtenna," *IEEE Antennas Wireless Propag. Lett.*, vol. 17, no. 8, pp. 1552–1556, Aug. 2018.
- [3] C.-T. Chuang and S.-J. Chung, "Synthesis and design of a new printed filtering antenna," *IEEE Trans. Antennas Propag.*, vol. 59, no. 3, pp. 1036–1042, Mar. 2011.
- [4] Y. Zhang, X. Y. Zhang, L.-H. Ye, and Y.-M. Pan, "Dual-band base station array using filtering antenna elements for mutual coupling suppression," *IEEE Trans. Antennas Propag.*, vol. 64, no. 8, pp. 3423–3430, Aug. 2016.
- [5] K. Xu, J. Shi, X. Qing, and Z. N. Chen, "A substrate integrated cavity backed filtering slot antenna stacked with a patch for frequency selectivity enhancement," *IEEE Antennas Wireless Propag. Lett.*, vol. 17, no. 10, pp. 1910–1914, Oct. 2018.
- [6] X. Y. Zhang, W. Duan, and Y.-M. Pan, "High-gain filtering patch antenna without extra circuit," *IEEE Trans. Antennas Propag.*, vol. 63, no. 12, pp. 5883–5888, Dec. 2015.
- [7] P. F. Hu, Y. M. Pan, K. W. Leung, and X. Y. Zhang, "Wide-/dual-band omnidirectional filtering dielectric resonator antennas," *IEEE Trans. Antennas Propag.*, vol. 66, no. 5, pp. 2622–2627, May 2018.
- [8] M.-C. Tang, B. Zhou, and R. W. Ziolkowski, "Flexible uniplanar electrically small directive antenna empowered by a modified CPW-feed," *IEEE Antennas Wireless Propag. Lett.*, vol. 15, pp. 914–917, 2016.
- [9] M.-C. Tang, B. Zhou, Y. Duan, X. Chen, and R. W. Ziolkowski, "Pattern-reconfigurable, flexible, wideband, directive, electrically small near-field resonant parasitic antenna," *IEEE Trans. Antennas Propag.*, vol. 66, no. 5, pp. 2271–2280, May 2018.